THE STARBURST GALAXY NGC 6090: AN ISO VIEW*

J.A. Acosta-Pulido[1,2,3], **U. Klaas**[2], **R.J. Laureijs**[1]

[1]ISO Data Centre, ESA Astrophysics Division, VILSPA, P.O. Box 50727, E-28080 Madrid, Spain
[2]Max–Planck–Institut für Astronomie, Heidelberg, Germany
[3]Instituto de Astrofísica de Canarias, E-38200 La Laguna, Spain.

ABSTRACT

We present ISOCAM and ISOPHOT observations of the galaxy pair NGC 6090. The SED derived from all ISO measurements is typical for strong starbursts which were triggered by the tidal interaction. With ISOCAM observations we could resolve the two nuclei of NGC 6090 separated by 6" in the MIR. The NE nucleus is the more active one, both in the optical and in the MIR.

Key words: ISO; infrared astronomy; galaxies; starburst; NGC 6090.

1. INTRODUCTION

NGC 6090 is a strongly interacting galaxy pair. The separation between the two nuclei is 6.4", which corresponds to a projected distance of 3.6 kpc (at a distance of 117 Mpc). It is classified as a Bright IRAS source, with an IR luminosity $\geq 10^{11}$L$_\odot$ (Soifer *et al.* 1987). The two nuclei show HII region like emission line spectra in the optical with similar extinction (E[B-V]$\sim$ 0.5) as determined from Balmer line ratios (Kim *et al.* 1995). The NE nucleus appears to be more active than the SW one: 2.2 and 3.7 times brighter in the B band and in Hα emission, respectively.

2. OBSERVATIONS

NGC 6090 was observed with ISOPHOT (Lemke *et al.* 1996) covering the full accesible wavelength range of this intrument (from 2.5 to 200 μm). The ISOPHOT data were reduced using the ISOPHOT Interactive Analysis (version 7.0). Results from the ISOPHOT data set were published earlier (Acosta–Pulido *et al.* 1996, hereafter paper I), here we present the data with improved calibration. Photometry in the 2.5–5.5 μm range was obtained by binning the ISOPHOT-SS channels to four wavelengths.

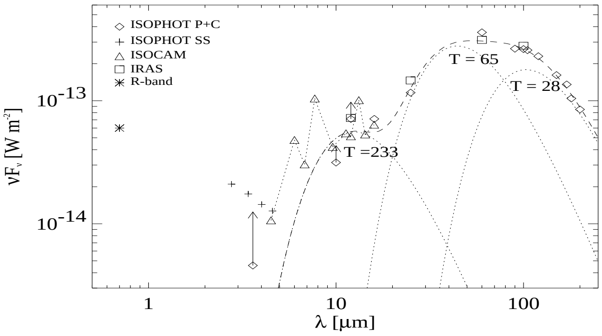

Figure 1. *Spectral energy distribution of NGC 6090. All ISO photometric data points are presented. The dashed line represents a composite model including three modified blackbody components. Photospheric stellar emission dominates at $\lambda \leq 4\mu m$.*

NGC 6090 was also observed with ISOCAM (Cesarky *et al.* 1996) using 10 filters from 4.5 to 15.5 μm, including two narrow band filters with the CVF in fixed mode. Our motivation for the ISOCAM observation was to provide spatial resolution to the feature emission we observed in the ISOPHOT-S spectrum. We performed a 3×3 microscanning raster using a step of 1/3 of a pixel in order to oversample the PSF. The pixel field of view was 3". Dark current subtraction and deglitching was done using standard CIA routines. A transient correction was performed using a procedure developed by ourselves based on the Fouks–Schubert transient model (Fouks *et al.* 1995). Different raster positions were combined using the drizzle algorithm (Hook & Fruchter, 1997), followed by a PSF deconvolution using the Lucy–Richardson algorithm within STSDAS/IRAF. We have used the theoretical PSFs provided within CIA (version 3.0).

3. RESULTS

3.1. Broad band photometry

The spectral energy distribution (SED) is shown in Fig. 1. The shape of the SED is well constrained

*ISO is an ESA project with instruments funded by ESA Member States (especially the PI countries: France, Germany, the Netherlands and the United Kingdom) and with the participation of ISAS and NASA.

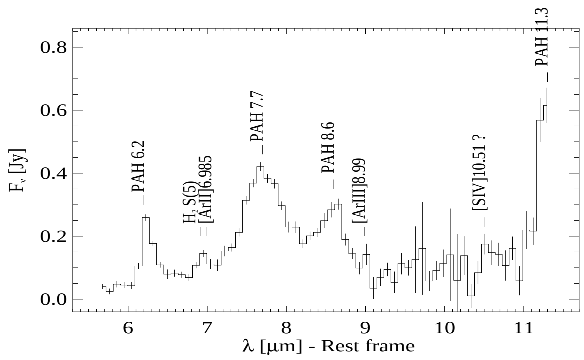

Figure 2. *ISOPHOT-SL spectrum of NGC 6090.*

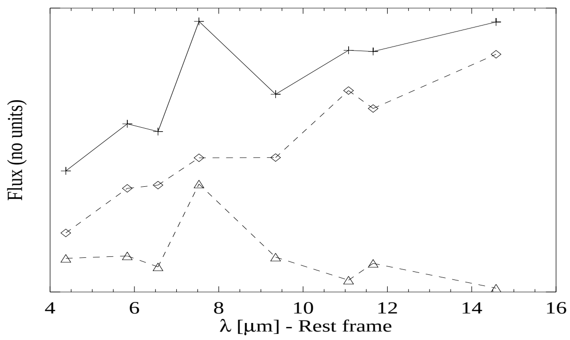

Figure 3. *NGC 6090 broad band spectra (F_ν) as measured through ISOCAM filters. The integrated spectrum is represented as crosses joined by a continuous line. Individual spectra corresponding to the NE and SW nuclei are represented by diamonds and triangles, respectively.*

by our multi–filter photometry, which sets strong requirements for modelling. From Fig. 1 it becomes clear that a substantial fraction (32%) of the IR energy is emitted at wavelengths shorter than 40 μm, not only in the form of continuum but emission in the broad features, as shown in Fig. 2. This emission is generally attributed to small grains and PAH emission. At $\lambda \leq 4$ μm the stellar photosphere emission dominates, as confirmed by the smooth transition from R–band ground based measurements (Huchra 1977) to ISOPHOT-SS data points (see Fig. 1).

We find that the IR continuum can be modelled in a first approach as the emission from three different temperature modified blackbody (emissivity $\propto \lambda^{-1}$) emission: a cold component of T$\sim$ 28 K, a warmer component of T$\sim$ 65 K and a hot component of T$\sim$ 233 K. This result is compatible with that found for other more luminous starburst galaxies (Klaas *et al.* 1997), and more surprisingly for Seyfert galaxies (Pérez García, Rodríguez Espinosa & Santolaya Rey, 1998). The hot component was fitted to the estimated underlying continuum, which makes it rather uncertain given the presence of emission features (see Fig. 2). In paper I we have shown that improved models containing PAH molecules are able to explain the observed SED in great detail (Krügel & Siebenmorgen, 1994).

3.2. Line Emission

We present in Fig. 2 our flux calibrated ISOPHOT-SL spectrum. In addition to the prominent PAH emission features, there is a clear detection of the following atomic lines: [ArII]6.98 μm + H_2S(5), [ArIII]8.99 μm, and less clear [SIV]10.5 μm. Emission from [NeII]12.81 μm and [NeIII]15.56 μm was measured using narrow band imaging (CAM–CVF), after continuum subtraction.

We have measured line ratios [NeIII]/[NeII] = 0.14 and [ArIII]/[ArII] = 0.56. These ratios are compatible with photoionization by photospheric emission of $T_{eff} \sim 38000$ K (Sellmaier *et al.* , 1996), and also typical of starburst galaxies (Spinoglio & Malkan, 1992).

3.3. MIR imaging

The separation of the two optical nuclei is very close to the maximum spatial resolution which can be achieved with ISOCAM. Our MIR imaging after mosaicing shows an elongated structure in all measured filters, however the two nuclei could be clearly resolved only after PSF deconvolution (see Fig 4).

Most of the MIR emission coincides with the nuclei, contrary to what was found for the Antennae galaxy (Vigroux *et al.* , 1996), which likely reflects different evolutionary stage in the two systems. The two nuclei show different MIR spectrum: the NE nucleus becomes dominant towards long wavelength, whereas the the SW one shows mostly PAH emission (see Figs. 3 and 5).

4. CONCLUSIONS

We present ISO photometry from 2.5 to 200 μm and MIR mapping of the starburst galaxy NGC 6090. The most remarkable results are the following:

- The SED is roughly the composition of 3 modified blackbody components with temperatures 233 K, 65 K and 28 K.
- Small grains and PAH molecules contribute to almost one third of the IR luminosity.
- Using ISOCAM the MIR emission from NGC 6090 could be resolved into two components (6" apart), corresponding to the location of the two optical nuclei.
- Most of the MIR emission is confined to the two optical nuclei. The NE nucleus is always dominant, whereas the SW nucleus becomes brighter at short wavelengths (4.5 μm) and when sampling PAH emission.

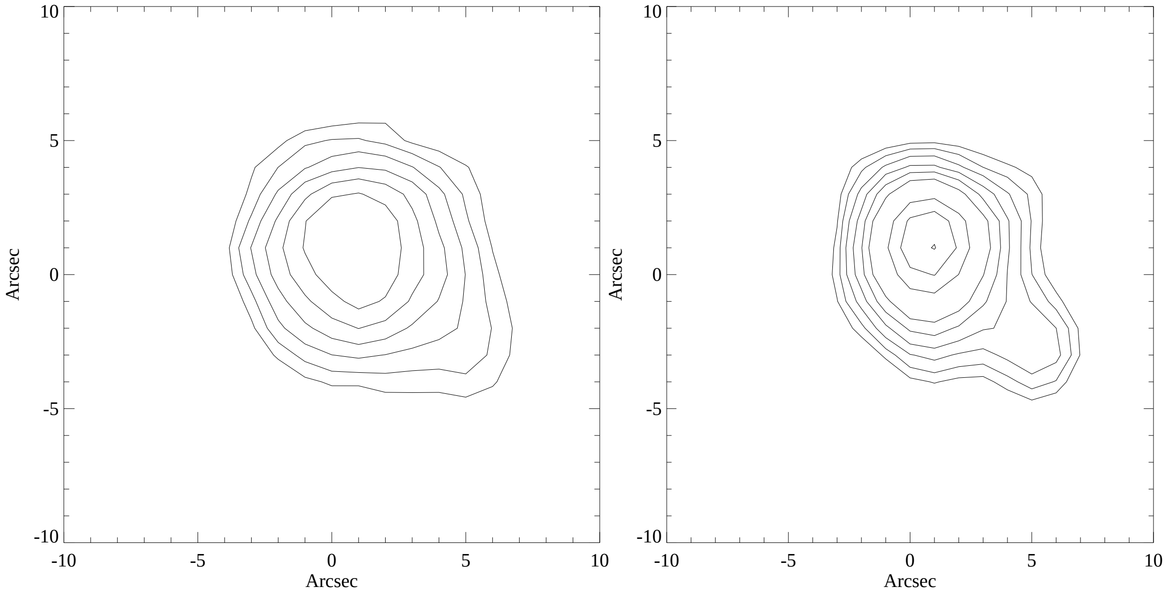

Figure 4. *NGC 6090 image corresponding to filter LW4 – 6 μm before (left panel) and after (right panel) PSF deconvolution. The orientation is N up and E to the left.*

ACKNOWLEDGEMENTS

It is a pleasure to acknowledge A. Biviano and B. Altieri for helping with the ISOCAM data analysis. The ISOPHOT data were reduced using PIA, which is a joint development of ESA Astrophysics Division and the ISOPHOT consortium. The ISOCAM data were reduced using CIA, which is a joint development of ESA Astrophysics Division and the ISOCAM consortium.

REFERENCES

Acosta–Pulido, J.A., Klaas, U., Laureijs, R.J., *et al.* 1996, A&A, 315, L121

Cesarsky, C.J. *et al.* 1996, A&A, 315, L32

Fouks, B.I. & Schubert J. 1995, Proc. SPIE, 2552, 421

Huchra, J.P. 1977, Ap.J.S., 35, 171

Hook, R. & Fruchter, A. 1997, ST-ECF Newsletter, 24, 9

Klaas, U., *et al.* 1997, A&A, 325, L21

Kim, D-C., *et al.* 1995, Ap.J.Supp., 98, 129

Krügel, E., & Siebenmorgen, R., 1994, A&A, 282, 407

Lemke, D., Klaas, U., Abolins J., *et al.* , 1996, A&A, 315, L64

Pérez Garcia A.M., Rodríguez Espinosa J.M. & Santolaya Rey A.E. 1998, Ap.J., 500, 685

Sellmaier, F.H., Yamamoto, T., Pauldrach, A.W.A. & Rubin, R.H., 1996, A&A, 305, L37

Soifer B.T., *et al.* 1989, A.J., 98, 766

Spinoglio L. & Malkan M. 1992, Ap.J., 399, 504

Vigroux L., *et al.* 1996, A.&A., 315, L93

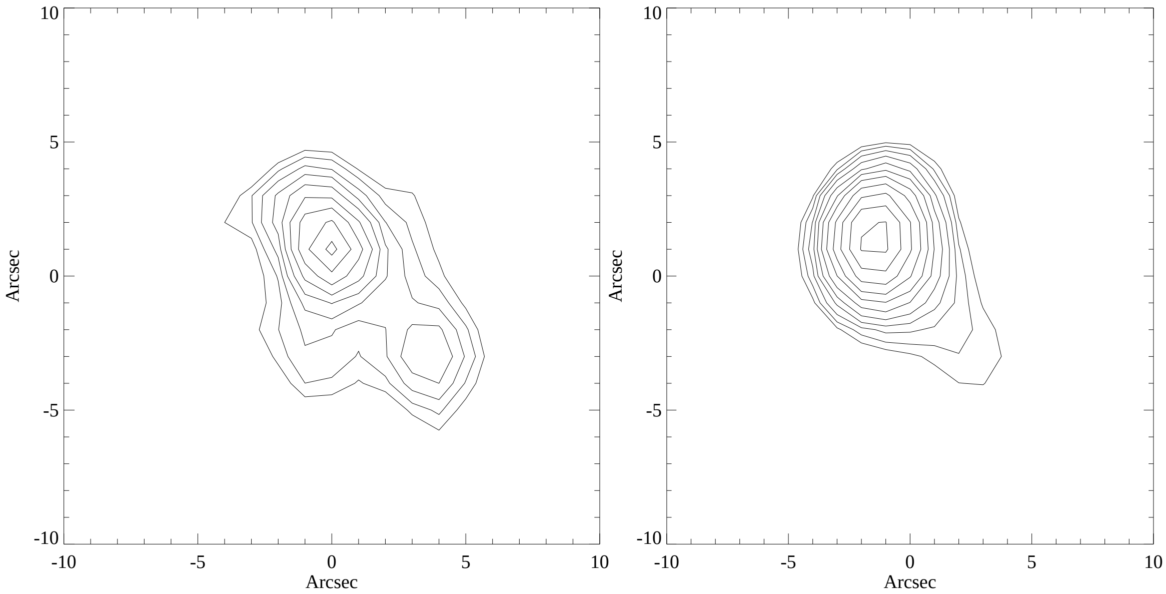

Figure 5. *NGC 6090 deconvolved images corresponding to filters LW1 – 4.5 μm (left panel) and LW3 – 14.3 μm (right panel). The orientation is N up and E to the left. The two nuclei contribute differently depending on the wavelength (see Fig. 3).*